



HAL
open science

Trapping of the Thioacylglyceraldehyde-3-phosphate Dehydrogenase Intermediate from *Bacillus stearothermophilus*

Sébastien Moniot, Stefano Bruno, Clemens Vornrhein, Claude Didierjean,
Sandrine Boschi-Muller, Mária Vas, Gerard Bricogne, Guy Branlant, Andrea
Mozzarelli, Catherine Corbier

► **To cite this version:**

Sébastien Moniot, Stefano Bruno, Clemens Vornrhein, Claude Didierjean, Sandrine Boschi-Muller, et al.. Trapping of the Thioacylglyceraldehyde-3-phosphate Dehydrogenase Intermediate from *Bacillus stearothermophilus*. *Journal of Biological Chemistry*, 2008, 283 (31), pp.21693-21702. 10.1074/jbc.M802286200 . hal-01690593

HAL Id: hal-01690593

<https://hal.univ-lorraine.fr/hal-01690593>

Submitted on 23 Jan 2018

HAL is a multi-disciplinary open access archive for the deposit and dissemination of scientific research documents, whether they are published or not. The documents may come from teaching and research institutions in France or abroad, or from public or private research centers.

L'archive ouverte pluridisciplinaire **HAL**, est destinée au dépôt et à la diffusion de documents scientifiques de niveau recherche, publiés ou non, émanant des établissements d'enseignement et de recherche français ou étrangers, des laboratoires publics ou privés.

Trapping of the Thioacylglyceraldehyde-3-phosphate Dehydrogenase Intermediate from *Bacillus stearothermophilus*

DIRECT EVIDENCE FOR A FLIP-FLOP MECHANISM*[‡]

Received for publication, March 24, 2008, and in revised form, May 13, 2008. Published, JBC Papers in Press, May 14, 2008, DOI 10.1074/jbc.M802286200

Sébastien Moniot^{‡1}, Stefano Bruno[§], Clemens Vornrhein[¶], Claude Didierjean[‡], Sandrine Boschi-Muller^{||}, Mária Vas^{**}, Gérard Bricogne[¶], Guy Branlant^{||}, Andrea Mozzarelli^{§††}, and Catherine Corbier^{‡§§2}

From the [‡]Laboratoire de Cristallographie et de Modélisation des Matériaux Minéraux et Biologiques, UMR CNRS-Université Henri Poincaré (UHP) 7036, the ^{||}Laboratoire de Maturation des ARN et Enzymologie Moléculaire, UMR CNRS-Université Henri Poincaré 7567, and the ^{§§}Unité de Recherche sur l'Animal et les Fonctionnalités des Produits Animaux, Équipe Protéolyse et Bio-fonctionnalités des Protéines et Peptides, EA 3998 Université Henri Poincaré, the Faculté des Sciences, Nancy Université, Vandoeuvre-lès-Nancy, 54506 Cedex, France, the [§]Department of Biochemistry and Molecular Biology and ^{††}Unit of the National Institute for Biostructures and Biosystems, University of Parma, Viale Usberti 23/A, Parma 43100, Italy, the [¶]Global Phasing Ltd., Sheraton House, Castle Park, Cambridge CB3 0AX, United Kingdom, and the ^{**}Institute of Enzymology, Biological Research Center, Hungarian Academy of Sciences, P. O. Box 7, Budapest H-1518, Hungary

The crystal structure of the thioacylenzyme intermediate of the phosphorylating glyceraldehyde-3-phosphate dehydrogenase (GAPDH) from *Bacillus stearothermophilus* has been solved at 1.8 Å resolution. Formation of the intermediate was obtained by diffusion of the natural substrate within the crystal of the holoenzyme in the absence of inorganic phosphate. To define the soaking conditions suitable for the isolation and accumulation of the intermediate, a microspectrophotometric characterization of the reaction of GAPDH in single crystals was carried out, following NADH formation at 340 nm. When compared with the structure of the Michaelis complex (Didierjean, C., Corbier, C., Fatih, M., Favier, F., Boschi-Muller, S., Branlant, G., and Aubry, A. (2003) *J. Biol. Chem.* 278, 12968–12976) the 206–210 loop is shifted and now forms part of the so-called “new P_i” site. The locations of both the O1 atom and the C3-phosphate group of the substrate are also changed. Altogether, the results provide evidence for the flipping of the C3-phosphate group occurring concomitantly or after the redox step.

Glyceraldehyde-3-phosphate dehydrogenase (GAPDH)³ is a homotetrameric enzyme catalyzing the oxidative phosphorylation of D-glyceraldehyde 3-phosphate (G3P) into 1,3-bisphos-

phoglycerate (1,3-DPG), in the presence of inorganic phosphate (P_i) and nicotinamide adenosine dinucleotide (NAD⁺).

The reaction mechanism has been intensively investigated in particular for bacterial and eukaryotic GAPDHs (1–9) and consists of two steps as follows: (i) an oxidoreduction reaction, corresponding to the nucleophilic attack of the catalytic cysteine (Cys-149) on the aldehydic group of G3P, followed by a hydride transfer assisted by His-176 (base catalyst) from the generated thiohemiacetal to the C4 of the nicotinamide of NAD⁺ that leads to the formation of a thioacylenzyme (7), and (ii) a phosphorylation of the resulting thioester through the nucleophilic attack of inorganic phosphate on the carbonyl group of the thioacylenzyme. The second step is preceded by the exchange of NADH with NAD⁺, with the latter favoring the phosphorylation step.

Two anion recognition sites accommodate the inorganic phosphate ion and the phosphate groups of G3P and 1,3-DPG. Their positions within the active site have been deduced from the location of two sulfate ions derived from the ammonium sulfate crystallization medium (9). On the basis of a model of the thiohemiacetal intermediate in the *Homarus americanus* GAPDH structure, the anion binding sites were initially attributed to the specific binding of the C3-phosphate (C3P) group of D-G3P (P_s site) and of the inorganic phosphate ion (P_i site). The location of the P_s site in the three-dimensional structures of eukaryotic and bacterial GAPDHs is conserved and independent of the enzyme state, apo-, or holo-form, and of the presence of ligands such as sulfate ions, phosphate ions, substrate, or substrate analogs. This P_s site is composed of the side chains of residues Arg-231 and Thr-179 and the 2'-hydroxyl group of the nicotinamide ribose of NAD⁺. On the contrary, the location of the P_i site appears to vary depending on the presence and nature of the bound ligands or source organism. This location is related to the conformation adopted by the segment composed of residues 206–212. Although the most common conformation is that originally found in the holoenzyme

* The costs of publication of this article were defrayed in part by the payment of page charges. This article must therefore be hereby marked “advertisement” in accordance with 18 U.S.C. Section 1734 solely to indicate this fact.

[‡] The on-line version of this article (available at <http://www.jbc.org>) contains supplemental Fig. S1.

The atomic coordinates and structure factors (code 3cmc) have been deposited in the Protein Data Bank, Research Collaboratory for Structural Bioinformatics, Rutgers University, New Brunswick, NJ (<http://www.rcsb.org/>).

¹ Fellow of the French Ministère de la Recherche et des Nouvelles Technologies.

² To whom correspondence should be addressed: Tel.: 33-3-83-68-42-67; Fax: 33-3-83-68-40-01; E-mail: catherine.corbier@scbiol.uhp-nancy.fr.

³ The abbreviations used are: GAPDH, D-glyceraldehyde-3-phosphate dehydrogenase (EC 1.2.1.12); G3P, D-glyceraldehyde 3-phosphate; 1,3-DPG, 1,3-bisphosphoglycerate; C3P group, C3-phosphate group; TAE, thioacylenzyme; r.m.s.d., root mean square deviation.

Thioacylenzyme Intermediate from *B. stearothermophilus* GAPDH

from *H. americanus* and *Bacillus stearothermophilus* (9–10), an alternative conformation was first observed in the holoenzyme from *Thermotoga maritima* and *Leishmania mexicana* (11–12) that generates a P_i site located closer to the catalytic Cys-149 residue and 3 Å away from the former position, which has been called new P_i site. Whatever the considered position, the P_i site includes the side chains of residues Ser-148 and Thr-208 and the main-chain nitrogen of Gly-209. In addition, the new P_i site also involves residue Thr-150.

Despite numerous functional (6, 7, 13) and structural studies (14–16), the individual role of P_i and P_s sites in the catalytic events remains unclear. Although it is generally assumed from geometrical considerations that inorganic phosphate must attack the intermediate from the P_i site, a possible flipping of the C3P of G3P between the two sites during catalysis was suggested by Skarzynski *et al.* (10).

Recently, using mutants of the active site cysteine, Didierjean *et al.* (16) obtained the structures of ternary complexes from *B. stearothermophilus* GAPDH with NAD^+ and the physiological substrate D-G3P, the phosphate group of which was found to be bound at the P_s site. This result strongly suggests that the P_s site constitutes the binding site for the C3P group of the substrate but does not, however, exclude the possibility that the substrate could display different interactions especially with regard to its C3P group, once the covalent bond is formed between Cys-149 and D-G3P. Indeed this structure is representative of a Michaelis, non-covalent, complex and does not allow to prefigure the location of the C3P group in the intermediate stages of the reaction.

Much of the uncertainty regarding the individual contribution of the two anion binding sites during the catalytic events derives from the absence of the structure of the physiological thioacylenzyme intermediate. To obtain this structure, holo-GAPDH crystals from *B. stearothermophilus* were soaked with the substrate G3P in the absence of inorganic phosphate. Formation of NADH in the crystal was monitored by single crystal absorption microspectrophotometry (17), a method pioneered by Rossi and Bernhard (18), for the determination of protein function in the crystalline state (19) and for the design of kinetic crystallography experiments (20). A series of microspectrophotometric studies on GAPDH crystals were previously carried out using a chromophoric substrate analog of 1,3-DPG (21–23). The experimental conditions suitable for the accumulation of the catalytically-relevant thioacylenzyme intermediate in the crystals of *B. stearothermophilus* GAPDH were thus designed and allowed us to solve its structure. This constitutes the first structure of a reaction intermediate of GAPDH in the presence of its cofactor NAD^+ . Analysis of the acylated structure reveals two major outcomes when compared with that of the non-covalent complex: a shift of the 206–210 loop, which delineates a new position for the P_i site comparable to that originally described for the holo-structure of *Thermotoga maritima*, and the location of the C3P group of the thioacyl intermediate, which is bound in this new P_i site.

EXPERIMENTAL PROCEDURES

Chemicals—DL-Glyceraldehyde-3-phosphate (DL-G3P, Sigma) was prepared from the DL-G3P diethylacetal according to the manufacturer, and its concentration was assessed using GAPDH. Iodoacetic acid, ammonium sulfate, EDTA, NAD^+ , Tris, and dithiothreitol were from Sigma and were of the best available quality and used without further purification.

Production, Purification, and Crystallization of Wild-type *B. stearothermophilus* GAPDH—The *Escherichia coli* strain used for wild-type GAPDH production was HB101 transformed with a pBluescript II SK containing the *gap* gene under the *lac* promoter. Purification was performed as previously described by Talfournier *et al.* (7). Purity of the enzyme was checked by electrophoresis on a 10% SDS-PAGE and by mass spectrometry.

Prior to crystallization, the enzyme was dialyzed overnight against 100 mM Tris buffer, pH 8.0, 2 mM EDTA, and 2 mM dithiothreitol, and concentrated using a 30-kDa molecular mass cut-off centrifugation system (Centricon). Protein concentration was determined spectrophotometrically at 280 nm using a molecular mass of 143,776 Da and an extinction coefficient of $1.31 \times 10^5 \text{ M}^{-1} \text{ cm}^{-1}$.

Crystals of the holo-form of wild-type *B. stearothermophilus* GAPDH were obtained at 293 K using the hanging-drop, vapor diffusion method in the presence of ammonium sulfate as precipitating agent. The reservoir solution contained 2.7 M ammonium sulfate, 100 mM Tris-HCl buffer, pH 6.9. Drops were prepared by mixing in different ratios a solution containing 15 mg·ml⁻¹ enzyme and 2 mM NAD^+ and the reservoir solution. Crystals appear within 1 week from drops with mixed volumes of protein and reservoir solutions in ratios of 1/2, 1/1, or 2/1.

Single Crystal-polarized Absorption Microspectrophotometric Measurements—Single crystals of GAPDH were resuspended at least six times in a stabilizing solution containing 2.7 M ammonium sulfate, 0.1 M Tris-HCl buffered at pH 8.2. Crystals were loaded in a quartz flow cell mounted on the stage of a Zeiss MPM03 microspectrophotometer, equipped with a 10× ultrafluar objective and a thermostatic apparatus (24). Polarized absorption spectra were recorded between 300 and 500 nm, with the electric vector of the linearly polarized light parallel to crystal edges.

To follow the reaction of GAPDH crystals with D-G3P, crystals were suspended in the stabilizing solution containing DL-G3P at concentrations up to 60 mM. Polarized absorption spectra were recorded as a function of time to monitor reaction equilibration. To obtain the reference spectrum for the fully reduced NADH-enzyme complex, single crystals were treated with 1 mM sodium arsenate in the presence of G3P. The arsenate anion irreversibly reacts with the thioacylenzyme, shifting the equilibrium toward the full reduction of NAD^+ . At each G3P concentration, the fraction of reduced NADH was calculated by fitting the corresponding absorption spectrum to a linear combination of the spectra of the native form and the arsenate-treated form. As a control experiment, enzyme crystals were suspended in a solution containing 10 mM iodoacetic acid, 2.7 M ammonium sulfate, 0.1 M Tris-HCl buffer, pH 8.2. This experiment was aimed to demonstrate the disappearance of the Racker band, diagnostic of an active enzyme, due to the

alkylation of the reactive Cys-149. All experiments were carried out at 15 °C.

X-ray Diffraction Experiments—Crystals of the holoenzyme were soaked for 1.5–10 min in a crystallization medium containing 60 mM DL-G3P. Reaction was stopped by flash freezing crystals after a quick soak in a cryoprotective solution containing 20% (v/v) glycerol in addition to the crystallization medium. Several datasets were collected at 100 K using a synchrotron beam either at European Synchrotron Radiation Facility (Grenoble, France) or Deutsches Elektronen-Synchrotron (Hamburg, Germany). 360 frames each of 0.5° oscillation step were systematically collected to assure collection of complete and redundant datasets, which were processed using the XDS package (25) and scaled using SCALA (26). The structure reported here (see below) derived from a crystal, soaked for 3 min, which diffraction data were collected at the X13 beamline (Deutsches Elektronen-Synchrotron) using a MARCCD detector (165 mm) and a wavelength of 0.806 Å. Statistics of the corresponding 1.77-Å resolution dataset are summarized in Table 1. Holo-crystals belong to monoclinic space group $P2_1$ with typical unit cell dimensions of $a = 82$ Å, $b = 123$ Å, $c = 82$ Å, and $\beta = 111^\circ$, containing one physiological homotetramer per asymmetric unit (as previously described by Skarzynski *et al.* (10)).

Phasing and Refinement—The structure was solved by molecular replacement using the MOLREP program (27) of the CCP4 suite (28) with the wild-type holo-structure (Protein Data Bank code 1gd1 (10)) as a starting model and data up to 3.6-Å resolution. Cycles of refinement (Refmac5) alternated with manual rebuilding (Coot) were carried out to improve the model (29, 30). Water molecules were added using the built-in find-water function of Coot and individually checked for significant signal and consistent contact with H-bond donor/acceptor. The thioacylenzyme model obtained from soaked ammonium sulfate-grown crystal was refined up to final convergence, using all the reflections (σ cut-off = 0) with R and R_{free} of 18.2% and 23.9%, respectively. The final cycles of refinement were performed using the BUSTER-TNT program (31), which allowed refinement of occupancy factors of the catalytic cysteine, reaction intermediate, 206–212 loop, and sulfate anions within the four monomers. This gave a final R and R_{free} of 16.1% and 19.8%, respectively.

Structure Analysis and Final Structure Parameters—The geometry of the model was checked with PROCHECK (32). Statistics concerning the geometry of the final model are given in Table 1. All non-glycine residues are located in favorable regions of the Ramachandran plot (33) except Asp-186 and Val-237, two residues already reported to be outside the allowed regions of the Ramachandran plot in the crystal structures of GAPDH isolated from *B. stearotherophilus* and other sources (34). The coordinates and structure factors of the thioacylenzyme structure have been deposited to the Protein Data Bank at Research Collaboratory for Structural Bioinformatics (ID code 3cmc). Figs. 2–4 were drawn with PyMOL.⁴

⁴ W. L. DeLano (2002) PyMOL, DeLano Scientific, San Carlos, CA.

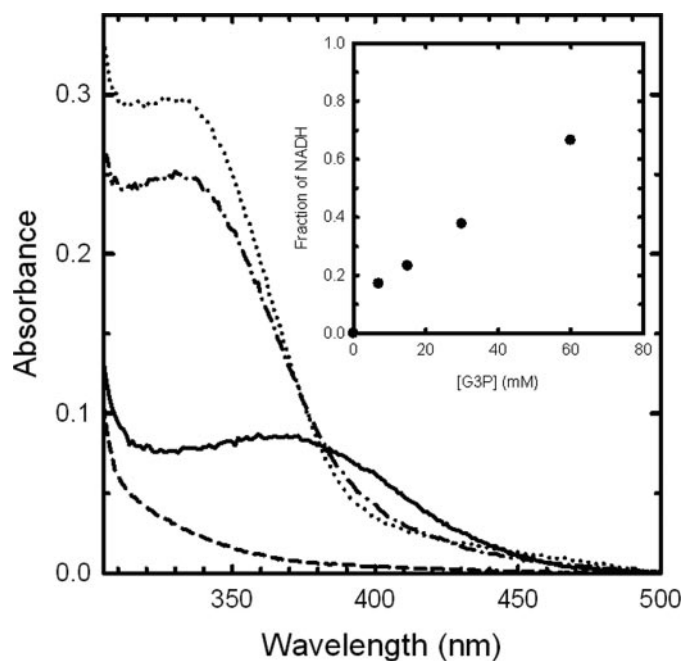


FIGURE 1. Polarized absorption spectra of single crystals of *B. stearotherophilus* holo-GAPDH in the absence and presence of G3P and iodoacetic acid. GAPDH crystals, grown in ammonium sulfate, were soaked in a stabilizing solution containing 2.7 M ammonium sulfate, 0.1 M Tris-HCl, buffered at pH 8.2 (solid line). The spectra were recorded with the light polarized perpendicular to the b axis of the crystal. The crystal was then resuspended three times with the same solution containing 10 mM iodoacetic acid (dashed line). Within the time required for the washing steps, a complete disappearance of the Racker band was observed. A different crystal was soaked with the stabilizing solution containing increasing concentrations of G3P (10, 15, 30, and 60 mM). The absorption spectrum obtained at 60 mM G3P is reported (dash-dot line). Further reduction of NAD^+ was obtained by soaking enzyme crystals with the stabilizing solution containing 60 mM G3P and 1 mM sodium arsenate (dotted line). The fractional reduction of NAD^+ by G3P was calculated at different G3P concentrations by fitting the observed spectra to a linear combination of the spectrum of the native form and the arsenate-treated form. *Inset:* dependence of the fractional reduction of NAD^+ as a function of G3P concentration (10, 15, 30, and 60 mM). Spectra recorded on different crystals were normalized using the spectrum of the holoenzyme as reference.

RESULTS

Polarized Absorption Spectra of *B. stearotherophilus* Holo-GAPDH Crystals in the Absence and Presence of G3P—Polarized absorption spectra of holo-GAPDH crystals from *B. stearotherophilus* grown in ammonium sulfate exhibited a broad band centered at around 360 nm (Fig. 1). This spectral feature, known as the Racker band, is associated with a charge transfer between the catalytic cysteine residue and the NAD^+ nicotinamide ring (35). Carboxymethylation of GAPDH crystals at the S γ of Cys-149 with iodoacetic acid resulted in the disappearance of the band (Fig. 1), as in solution, indicating that GAPDH in the crystal is in a catalytically active conformation. A similar observation was obtained on GAPDH crystals from *Palinurus vulgaris* (21).

Upon addition of the physiological substrate G3P to holoenzyme- NAD^+ crystals, an intense band centered at around 340 nm, associated with the formation of NADH , appeared with the concomitant disappearance of the Racker band (Fig. 1). This result indicates that the redox reaction has occurred in the crystalline state, with the hydride transfer from C1 of G3P to C4 of nicotinamide ring and concom-

Thioacylenzyme Intermediate from *B. stearothermophilus* GAPDH

itant formation of the thioacylenzyme-NADH complex, as observed in solution (2–3, 36). The reduction of all four NAD⁺ molecules of the tetramer could be achieved by adding sodium arsenate to the soaking solution containing G3P (Fig. 1). The arsenate anion irreversibly reacts with the acylenzyme, thus shifting the equilibrium toward the reduction of NAD⁺. The fraction of acylated sites and NADH molecules depends on the concentration of G3P in the soaking solution (Fig. 1, *inset*). A titration of GAPDH crystals with increasing concentrations of G3P revealed a relatively low apparent affinity for GAPDH with respect to solution (Fig. 1, *inset*), likely due to the inhibitory effect of the high sulfate concentration in the suspending medium, competing for the anion binding sites. Indeed, a similar behavior was observed for *P. vulgaris* GAPDH crystals, grown in ammonium sulfate (data not shown), whereas on the contrary, crystals of *B. stearothermophilus*, grown from polyethylene glycol solutions, reacted with G3P with complete reduction of NAD⁺ at ~1 mM G3P (data not shown). However, the reaction of G3P with these polyethylene glycol-grown

GAPDH crystals was systematically accompanied by a significant decrease of the diffraction power, preventing their use for structural determination.

Overall Structure and Model Quality—The final model is composed of one tetramer in the asymmetric unit, each monomer containing residues 0–333 and one molecule of cofactor. The asymmetric unit also contains 4 bound G3P molecules, 18 sulfate ions (including two in each active site), 8 molecules of glycerol, and 1 molecule of ethylene glycol derived from the cryoprotective treatment (see “Experimental Procedures”) and 1743 water molecules. Except for some solvent-exposed side chains, residues of the model are well defined in the electron density maps. Only a few residual peaks, mostly in the solvent-exposed region, were not interpreted in the difference maps. The model has tight stereochemical restraints with r.m.s.d. on bond lengths and on bond angles of 0.011 Å and 1.27°, respectively (Table 1).

The four monomers are named O, P, Q and R, following the nomenclature initially described for *H. americanus* GAPDH (37). Using the O subunit as a reference, the root-mean-square deviations (r.m.s.d.) of backbone atoms after superimposition of the P, Q, and R subunits are 0.15, 0.14, and 0.12 Å, respectively, showing that the conformations of all four subunits in the final refined tetramer are very similar. Superimposition of the backbone atoms of our model onto the holo-structure described by Skarzynski *et al.* (10) (same space group and unit cell dimensions; pdb code 1gd1) gives an r.m.s.d. of 0.45 Å for the whole tetramer and a mean value of 0.27 Å for the different pairwise superimpositions of the monomers. No major difference was observed between the two structures except locally for the 206–212 loop, which exhibits deviations three times higher than the r.m.s.d. This conformational difference will be further described below.

As expected from the stoichiometry of the reaction of GAPDH crystals with 60 mM DL-G3P (fraction of NADH per monomer of ~0.70), determined by polarized absorption microspectrophotometry (Fig. 1, *inset*), the active site of each subunit was found to be present in two distinct, differently populated chemical states, which have been assumed to correspond to the native holo-structure with a free cysteine and a sulfate anion bound to the P_i site (mean refined fractional occupancy of ~0.4, conformation A) and to the thioacylenzyme-NADH intermediate (mean refined fractional occupancy of ~0.6, conformation B) (Table 2). The refined occupancies and B values of the ligands are similar in the four monomers and support an equivalent distribution of the thioacylenzyme intermediate in all subunits. The differences between the two states are also

TABLE 1
Data collection and refinement statistics

Values in parentheses refer to the outermost resolution shell.

Thioacylenzyme structure (soaked ammonium sulfate crystal)	
Data collection	
Space group	P2 ₁
Unit cell (Å)	<i>a</i> = 81.7; <i>b</i> = 122.6; <i>c</i> = 81.8; β = 111.1
Z	2
Nominal resolution (Å)	1.77
Outermost resolution shell (Å)	1.88–1.77
Temperature (K)	100
Unique reflections	142,733 (20,259)
Completeness (%)	97.7 (92.9)
Redundancy	3.7 (3.2)
<i>R</i> _{merge} ^a (%)	2.8 (18.9)
Mean I/ σ (I)	32.1 (6.5)
Refinement	
<i>R</i> -factor ^b (%)	16.1
<i>R</i> _{free} ^c (%)	19.8
r.m.s.d. from ideal geometry	
Bond lengths (Å)	0.011
Bond angles (°)	1.27
Dihedral angles (°)	17.0
Improper angles (°)	26.0
Mean <i>B</i> -factor (Å ²)	
Overall model	25.7
Protein atoms	23.6
NAD	17.1
Reaction intermediate	27.4
Sulfate atoms	40.4 (45.8–34.7)
(P _i and P _s site sulfates)	
Water molecules	37.7

^a *R*-factor for symmetry-related intensities.

^b Crystallographic *R*-factor.

^c Crystallographic *R*-factor for a randomly selected 5% of reflections not included in refinement.

TABLE 2
Occupancy factor refinement and thermal agitation values

Subunit		O	P	Q	R
Thioacyl intermediate	Refined occupancy	0.64	0.59	0.62	0.67
	Mean <i>B</i> value (Å ²)	27.3	27.9	26.8	27.6
	Real space correlation coefficient ^a	0.95	0.91	0.94	0.94
Sulfate (P _i site)	Occupancy	0.33	0.47	0.41	0.27
	<i>B</i> value (Å ²)	46.1	45.6	45.1	46.3
206–212 loop (confA/confB)	Refined occupancy	0.47/0.53	0.66/0.34	0.65/0.34	0.44/0.56
	Mean <i>B</i> value (Å ²)	24.8/25.6	24.5/25.2	23.8/24.5	24.9/25.5
	Real space correlation coefficient ^a	0.93/0.87	0.95/0.90	0.95/0.89	0.94/0.88

^a Correlation existing between model density and $2mF_o - DF_c$ density.

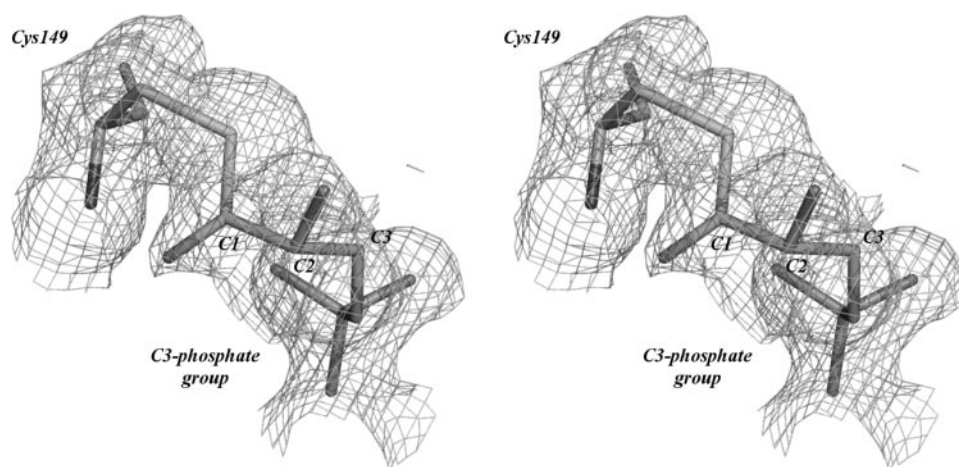


FIGURE 2. **Stereoscopic view of the thioacylzyme intermediate (subunit O).** The catalytic cysteine (Cys-149) and the bound substrate are presented in stick mode in $2mF_o - DF_c$ omit maps contoured at 1σ . These maps were obtained by removing from the model all atoms of the protein, NAD, sulfate, and water molecules within 3.6 \AA of the thioacylzyme intermediate residues. This omit model was refined again with Buster, eliminating the excluded regions also from the bulk solvent part of the model. Continuity of the density covering all atoms of the substrate is satisfying especially regarding the relatively low occupancy of these atoms (0.64). Note the trans conformation retained by the two oxygen atoms bound to C1 and C2, respectively.

reflected in the 206–212 loop that was built in the electron density maps in two alternate conformations, A and B, each associated with one of the two states presented above. Refinement of the occupancies of both 206–212 loop alternate conformations shows the existence of two subunit types. O and R subunits exhibit almost equal occupancies for the two conformations, whereas the native conformation is prevailing in P and Q (Table 2). Although this loop is not directly involved in crystal packing, such difference could arise from the distinct crystalline environment of each subunit extensively described by Skarzynski *et al.* (10). Despite these slight occupancy variations, conformations of the 206–212 loop and of bound ligands are similar in the four monomers. Therefore, all following descriptions and comparisons, except when specified, will be based on the structure of the O monomer.

Conformation of the Thioacyl-GAPDH-NADH Intermediate—The thioacylzyme intermediate is present in each subunit with a refined occupancy factor varying from 0.59 to 0.67. It is well defined with good connectivity in monomers O and R and a real space correlation coefficient of 0.94 (Table 2 and Fig. 2). In monomers P and Q, density is poorer with a lack of signal at the C2 atom level (Table 2 and supplemental materials). Although no NCS restraints were applied on the bound substrate, the conformation of the intermediate and the interactions shared with the protein structure are almost identical in the four monomers.

The 3-phosphoglyceroyl moiety is bound via a planar thioester bond formed between the sp^2 C1 atom and the $S\gamma$ atom of the catalytic cysteine (Cys-149) (Fig. 2). The plane of the thioester bond is almost parallel to the one defined by the nicotinamide ring, and the carbonyl oxygen (O1) points in a direction opposite to the catalytic His-176 to accept a H-bond from the Cys-149 main chain and from a water molecule (Fig. 3A). Whereas DL-G3P was used for soaking experiments, the C-2 carbon is found in an R configuration, which accounts for the enantiomer specificity of the GAPDH enzyme toward D-G3P

(38). The C2 hydroxyl group points away from the carbonyl group at C1 to adopt a trans conformation. The O2 oxygen atom is assumed to form H-bonds with both the NO7 atom of the cofactor and with the Ne atom of His-176. The C3P group is located in the new P_i site, formed by the 206–212 loop under its B conformation (see below). Its oxygen atoms are hydrogen-bonded to the side chains of Ser-148, Thr-150, and Thr-208 and to the main chain of Thr-150 and Gly-209, all of these residues being invariant. Additional interactions are provided by the non-conserved Arg-195 and by the invariant Arg-231 via two water molecules (see Table 3 for interaction distances).

Given the refined fractional occupancy of this intermediate (Table 2),

one has to assume that Cys-149 also exists in its free state. Based on the shape of the density map and on refinements, this residue was built under a unique conformation that is representative of both states. The side chain of the catalytic cysteine superimposes perfectly with that of the known holo-structure from *B. stearothermophilus*. In its free form, this side chain is well positioned to form an ion pair with the Ne atom of His-176 distant of 3.6 \AA .

In each monomer, the cofactor molecule is well defined in density maps with full occupancy. Because the reaction with G3P in the crystal was not complete, a mixture of oxidized and reduced forms is expected for the cofactor. However, the two redox states cannot be distinguished from the 1.77-\AA electron density map, and there is no evidence to support any change of conformation for the cofactor molecule after hydride transfer.

A sulfate ion is bound with full occupancy in the P_s site through five hydrogen bonds to Arg-231, Arg-195, and Thr-179 side chains, the 2'-OH atom of the ribose adjacent to the nicotinamide, and a water molecule (Fig. 3A). A second sulfate ion is located in the P_i site with partial occupancy (see above). It interacts with the side chains of Thr-208 and Ser-148 and with the main-chain N atom of Gly-209 (conformation A of the 206–212 loop). This anion exhibits a high B value (45.8 \AA^2) in comparison with the model mean value (25.7 \AA^2) and is poorly defined in electron density maps. However, a water molecule cannot account for the observed electron density, and the location of this anion matches the one bound in the P_i site of the holoenzyme structure (10).

Alternate Conformations of the 206–212 Loop—Delineating one side of the active site, the 206–212 loop contributes to the formation of one of the two anion binding sites. As mentioned above, this loop has been unequivocally fitted into the density maps under two conformations (Fig. 4A and Table 2). The first conformation, called conformation A, is strictly equivalent to the conformation described in the holo-structure (10, 16). In this conformation, the loop participates in the binding of a sul-

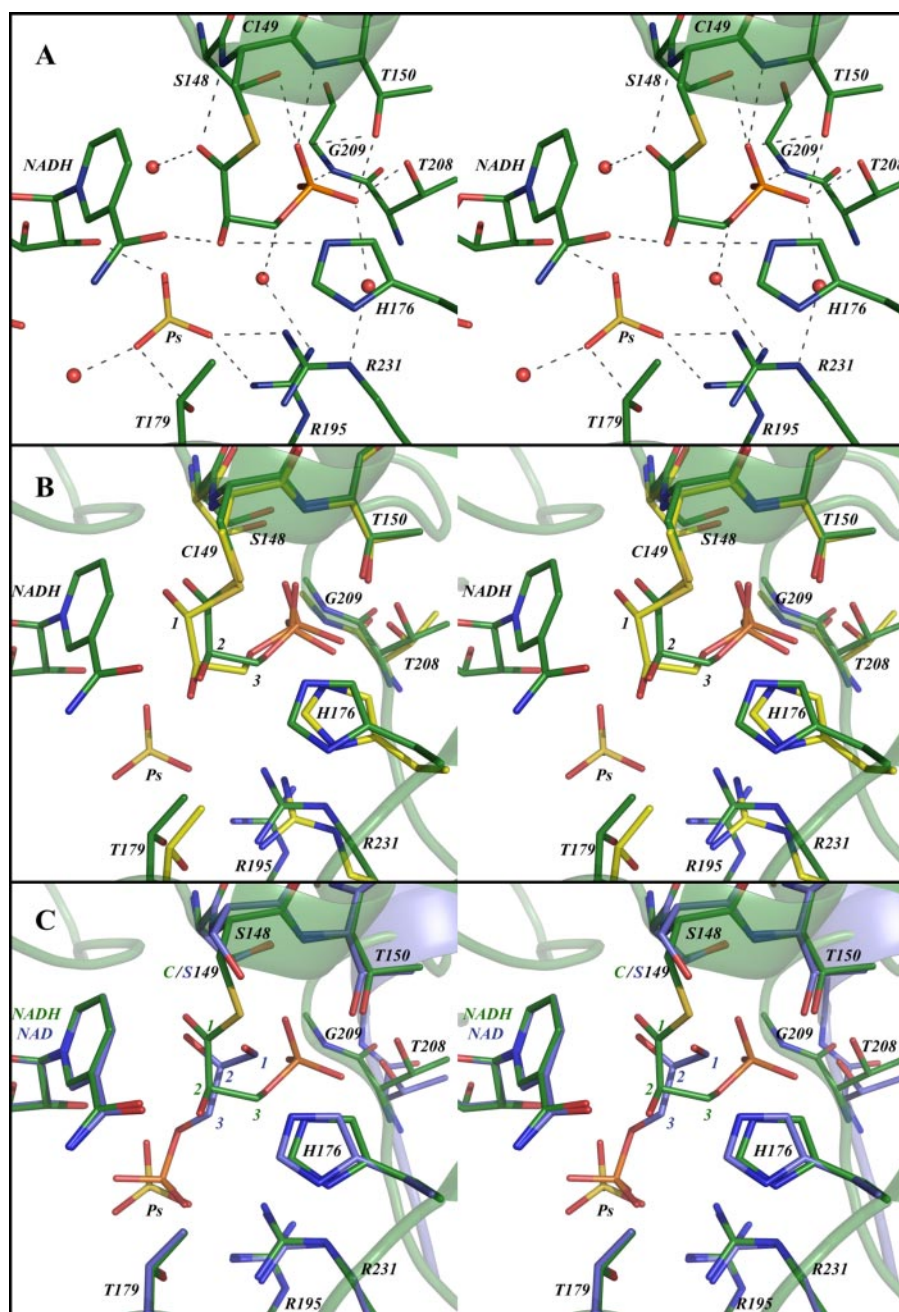


FIGURE 3. Active site and comparison with other representative complexes. The reaction intermediates, the substrate and cofactor molecules, and the residues involved in catalysis and substrate binding are presented in *stick mode*. Labels 1, 2, and 3 refer to the C1, C2, and C3 atoms of the substrate, respectively. *A*, stereoscopic view of the active site of the thioacyl intermediate structure. Hydrogen bonds are presented as *dashed lines*. Important water molecules are shown as *spheres*. *B*, stereoscopic view of the superimposition between this model (*green*) and the hemithioacetal structure of *E. coli* apo-GAPDH (*yellow*) (1DC4) (14). *C*, stereoscopic view of the superimposition between this model (*green*) and the Michaelis ternary complex from *B. stearothermophilus* holo-GAPDH (C149S mutant, in *blue*) (1NQO) (16).

fate anion in the “classic” P_i site. The second conformation of the loop (conformation B), with complementary occupancy, displays a maximum shift of 3.4 Å for the Gly-209 $C\alpha$ atom toward the catalytic cysteine. In this alternate position, the 206–212 loop is located too close to the sulfate molecule to allow both of them to coexist in the same position, confirming that the presence of the sulfate anion is associated with the above described loop conformation A (Fig. 4A). The loop in conformation B is very similar to the one initially described for

T. maritima GAPDH (see Fig. 4B) (11) and contributes to the formation of the anion binding site called new P_i . Both conformations have nearly identical thermal motion factors (24.5 and 25.2 Å², for conformations A and B, respectively), which fall in the same range of the overall protein (23.6 Å²), suggesting that both states of the 206–212 loop are stable conformations.

Comparison with Other Structures—The position of the new P_i binding site, here observed for the first time in *B. stearothermophilus* GAPDH, is equivalent to that described for structures of GAPDH from other sources (11–12, 14). Superimposition of the main-chains atoms of the O subunit of our model with those of the hemithioacetal structure of *E. coli* apo-GAPDH (pdb code 1dc4, A chain (14)) locates the two phosphorus atoms only 0.33 Å away from each other (Fig. 3B). As well, the central atoms of the sulfate and phosphate anions bound in the new P_i site of *T. maritima* (pdb code 1hdg, O chain (11)) and *L. mexicana* (pdb code 1gyp, A chain (12)), respectively, after similar superimposition procedures, are situated only 0.17 and 0.42 Å away from the phosphorus atom of the thioacylzyme intermediate, respectively. The position and geometry of the substrate in this intermediate are very close to those described by Yun *et al.* (14) for the hemithioacetal structure (pdb code 1dc4) of *E. coli* apo-GAPDH. Only a slight shift can be observed between the two bound G3P molecules (Fig. 3B) that can be related, first, to the different hybridizations of the two C1 atoms, and second, to the steric influence of the cofactor molecule, which is missing in the hemithioacetal apostructure. As previously

described by Yun *et al.* (14) for the hemithioacetal intermediate, the oxygen bound to C1 points away from the hydroxyl group of C2 to adopt a trans conformation. Thus, the O1 atom of G3P turns away from the catalytic His-176 in a counterintuitive manner with respect to its demonstrated catalytic role (see “Discussion”).

When the thioacyl-GAPDH structure is compared with the non-covalent Michaelis complex obtained by Didierjean *et al.* (16) for *B. stearothermophilus* GAPDH (pdb code 1nqo), the

TABLE 3

Substrate-protein interactions

Numbers in parentheses refer to the water molecule numbers as defined in the atomic coordinate file.

	O	P	Q	R
			Å	
O1-G3P-N-Cys-149	2.7	2.6	2.7	2.7
O1-G3P-H ₂ O	3.0 (W558)	2.7 (W1547)	3.0 (W1056)	2.7 (W1213)
O2-G3P-NO7-NAD	2.7	2.7	2.7	2.8
O2-G3P-Nε-His-176	3.1	3.1	3.2	3.1
O1P-G3P-H ₂ O	3.0 (W395)	3.0 (W631)	2.9 (W1743) 3.0 (W367)	3.0 (W111)
O2P-G3P-N-Gly-209	2.3	2.4	2.4	2.5
O2P-G3P-H ₂ O	/	/	3.2 (W367)	3.1 (W111) 3.1 (W1701)
O3P-G3P-Oγ ₁ -Thr-150	2.6	2.5	2.5	2.5
O3P-G3P-Oγ ₁ -Thr-208	2.7	2.8	2.9	2.7
O3P-G3P-H ₂ O	2.8 (W181)	2.7 (W253)	2.6 (W189)	2.8 (W216)
O4P-G3P-Oγ-Ser-148	3.0	3.0	3.2	2.9
O4P-G3P-N-Thr-150	2.9	3.1	3.0	3.0
O4P-G3P-Oγ ₁ -Thr-150	2.7	2.8	2.6	2.7

main difference concerns the binding of the C3P group, which is located in the P_s site in the non-covalent complex (Fig. 3C), ~6 Å away from the new P_i site. This shift of the C3P group is also accompanied by a complete rearrangement of the carbon chain, which results in significant modifications of its interaction pattern with the protein. Thus, the orientations of the C1–O1 and C2–O2 bonds differ drastically in the two structures. Although the O1 atom points toward the catalytic histidine and the C2–O2 bond is almost perpendicular to the nicotinamide ring in the Michaelis complex, the O1 atom points away from the histidine and the C2–O2 bond is almost parallel to the nicotinamide ring in the thioacylenzyme.

DISCUSSION

This report presents for the first time the crystal structure of a thioacylenzyme intermediate of GAPDH. The strategy used to obtain this intermediate takes advantage of the slow rate of the deacylation step in the absence of phosphate ions. Under this condition, the rate of hydrolysis of the intermediate is 10⁻² s⁻¹, i.e. 6 × 10⁴ times slower than acylation (6), which allows the intermediate to accumulate in the crystal. Despite the partial occupancy of the intermediate, the quality of the diffraction data and of the resulting structure allowed us to build two distinct states of the enzyme, which are each present in the four monomers of the enzyme. The most populated state corresponds to the structure of the thioacylenzyme intermediate covalently bound to the catalytic cysteine and the other one corresponds to a state in which the catalytic cysteine is free and a sulfate ion is bound in the classic P_i site. Each state is associated with a particular conformation of the 206–212 loop in which invariant Thr-208 and Gly-209 interact with either the C3P of the thioacyl intermediate or a sulfate anion.

Structure of the Thioacylenzyme Intermediate and Implications for Catalysis—The phosphate group of the thioacyl intermediate is bound in the new P_i site. This result is consistent with the location of the substrate phosphate group found in the structure of the hemithioacetal (*sp*3) intermediate obtained with the apo-GAPDH from *E. coli*: the two structures superimpose well (Fig. 3B) except at C1 due to different hybridization (*sp*2 instead of *sp*3). On the other hand, structures considered to be representative of a productive enzyme-NAD-D-G3P non-covalent complex (16) showed that the P_s site constitutes the binding site for the C3P group of the substrate in this Michaelis

complex. Taken altogether, these results suggest that, even in the presence of a fully formed P_s site (presence of the ribose of the cofactor to interact with the P_s site, a condition that was not fulfilled for the hemithioacetal structure from *E. coli* GAPDH in which the enzyme was under its apo-form), the C3P group of the substrate has shifted from P_s site to the new P_i site during the oxidoreduction step. The exact stage at which this shift occurs remains unknown. However, although one cannot rule out the possibility that the formation of the covalent bond between Cys-149 and D-G3P promotes the repositioning of the C3P in the new P_i site, it seems more likely that the first step of the reaction occurs while the C3P group is bound at the P_s site and that the relocation of the phosphate group occurs once hydride transfer is achieved. Indeed, a hydride transfer, while the C3P group is still bound at P_s, would present the advantage of holding both the substrate and cofactor in tight interaction and might promote this step of the reaction.

Besides the C3P group location, an unexpected feature concerns the orientation of the oxygen atom bound at C1, which points opposite to His-176, almost parallel to the nicotinamide ring (Fig. 3A), and adopts an energetically favorable trans conformation when related to the O2 atom position. It is well established that an efficient hydride transfer requires either a base-catalyst or an oxyanion hole to stabilize the negative charge developed on the tetrahedral transition state. Whereas non-phosphorylating GAPDHs possess the geometric features of an oxyanion hole reminiscent to those from serine proteases (39), these criteria are clearly not fulfilled in phosphorylating GAPDHs. His-176 was shown instead to play an unequivocal role of base-catalyst during the redox step (5, 7). This means that hydride transfer must have occurred with the C1-OH group well oriented with respect to His-176. In the structure presented here, which is representative of a stage after hydride transfer, the oxygen atom at C1 adopts another position that results in the disruption of the alignment between the Nε atom of His-176, the O1 and C1 atoms of the substrate, the hydride ion, and the C4 atom of the pyridinium ring.

It appears thus that the overall redox step involves important conformational adjustments of the substrate and requires the relocation of both O1 atom that shifts away from His-176 and of the C3P group that flips from the P_s site toward the new P_i site. Whether these two events are coupled or not is still unclear.

Thioacylenzyme Intermediate from *B. stearothermophilus* GAPDH

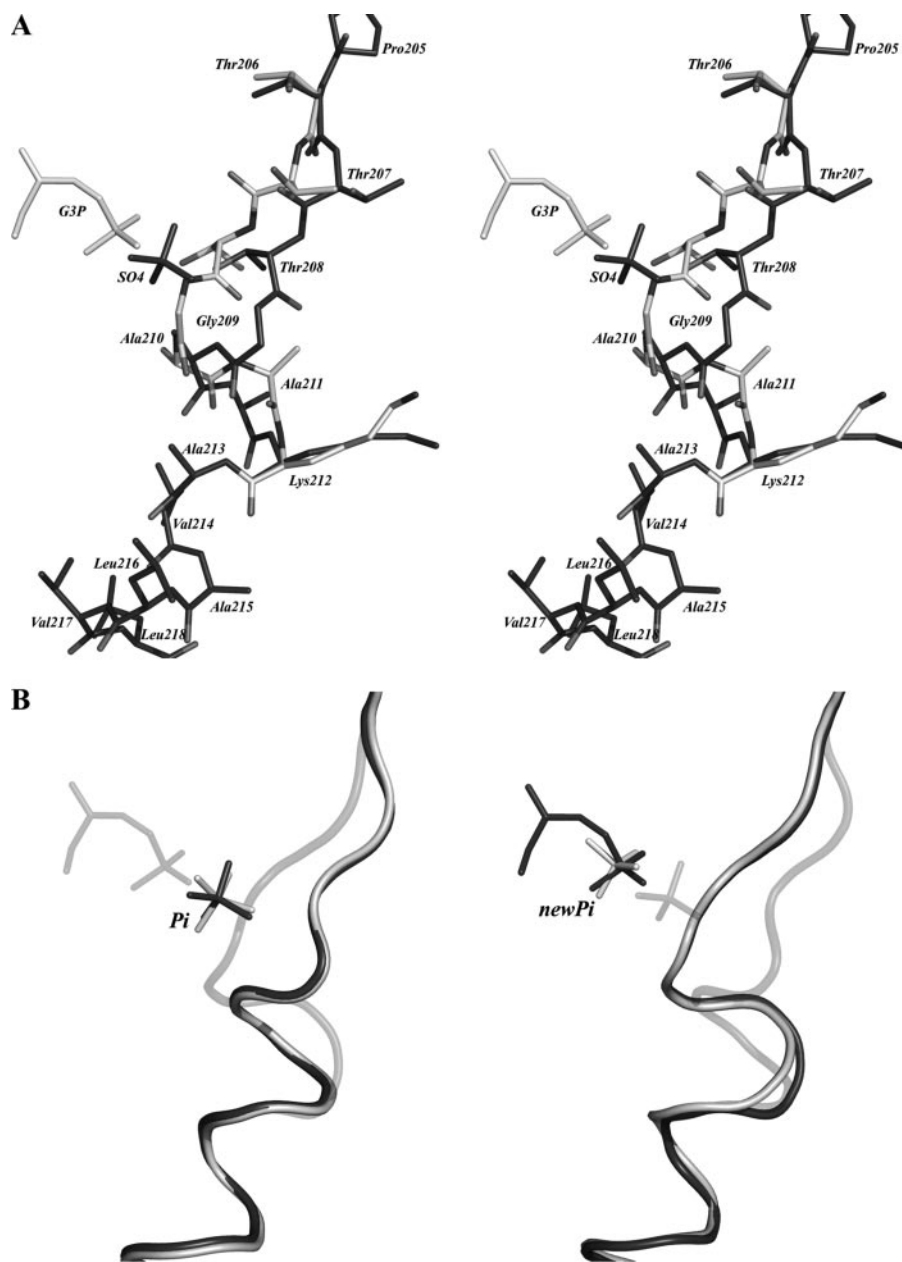


FIGURE 4. Alternate conformations of the 206–212 loop and re-location of the P_i anion binding site. *A*, stereoscopic view of the O subunit region spanning residues 205–218. The 206–212 loop is represented in two alternate conformations: in *dark gray*, the classic conformation delineates the P_i anion binding site where a sulfate is bound (conformation *A*). In *light gray*, the alternate conformation exhibits a shift toward the C3P of the intermediate (conformation *B*). This motion allows Thr-208 and Gly-209 to participate to the formation of the new P_i site and thus to the binding of the C3P group of the intermediate. *B*, superimposition of the 206–212 loop with representative GAPDH structures. The superimposition of the 206–212 loop under its classic conformation (*dark gray*) with the holo-structure from *B. stearothermophilus* (in *white*, pdb code 1gd1 (10)) is reported on the *left*, and the superimposition of the 206–212 loop under its alternate conformation with the structure of *T. maritima* GAPDH (in *white*, pdb code 1hdg (11)) is reported on the *right*. All structures are represented in *schematic mode* with their corresponding bound anion in *stick mode*. To facilitate comparison, both conformations of our model were represented in each superimposition, *shading* the one that is not considered.

However, the fact that both relocations seem to occur at the same stage, that is once hydride transfer is achieved, strongly suggests these two events to be coupled. One should note that, except for the 206–212 loop, the active site conformation remains unchanged between the Michaelis complex and the thioacylenzyme intermediate structures and that only the substrate conformation is modified along the redox step. The path-

way leading from one conformation to the other implies mainly a rotation of the trans plane O1–C1–C2–O2 of $\sim 180^\circ$. A rotation around the C2–C3 bond is also needed for the adequate positioning of the C3P group in the new P_i site.

The next step consists of the release of the cofactor NADH, which was shown to be rate-limiting in the overall enzymatic process, and the entry of a new molecule of NAD^+ , which is known to enhance the rate of phosphorolysis (2).⁵ The events promoting NADH release are still unclear. However, the loss of the interaction between O2' of the ribose and the C3P group of the intermediate following the flipping of the C3P group from the P_s site to the new P_i site could be the first signal that triggers the dissociation of NADH. Note that, although a mixture of NAD^+ and NADH is present in the structure (due to an incomplete reaction), the two states cannot be distinguished from the electron density maps and have been built as one conformation. Therefore, except for the above mentioned point, no evidence exists in the structure that might account for a destabilization of the cofactor-enzyme complex.

The entry of a new NAD^+ molecule likely promotes conformational changes on the substrate molecule required for phosphorolysis. Indeed, taking into account the facts that (i) His-176 has to play a role as an acid/base catalyst (10) in the phosphorolysis step as it does in the acylation step and (ii) the inorganic phosphate has to bind to either the classic P_i (10) or the new P_i site (12), the consequence of the re-entry of NAD^+ should be a flip back of both the O1 atom and the C3P groups to their initial position to interact with His-176 (Ne) and to bind to the P_s site, respectively. Again, these rearrangements can be coupled or occur in two distinct steps.

Proposed Scenario—G3P initially binds to the active site with its C3P located in the P_s site. Reaction begins through the nucleophilic attack of the Cys-149, whose thiol function is first

⁵ F. Talfournier, unpublished results.

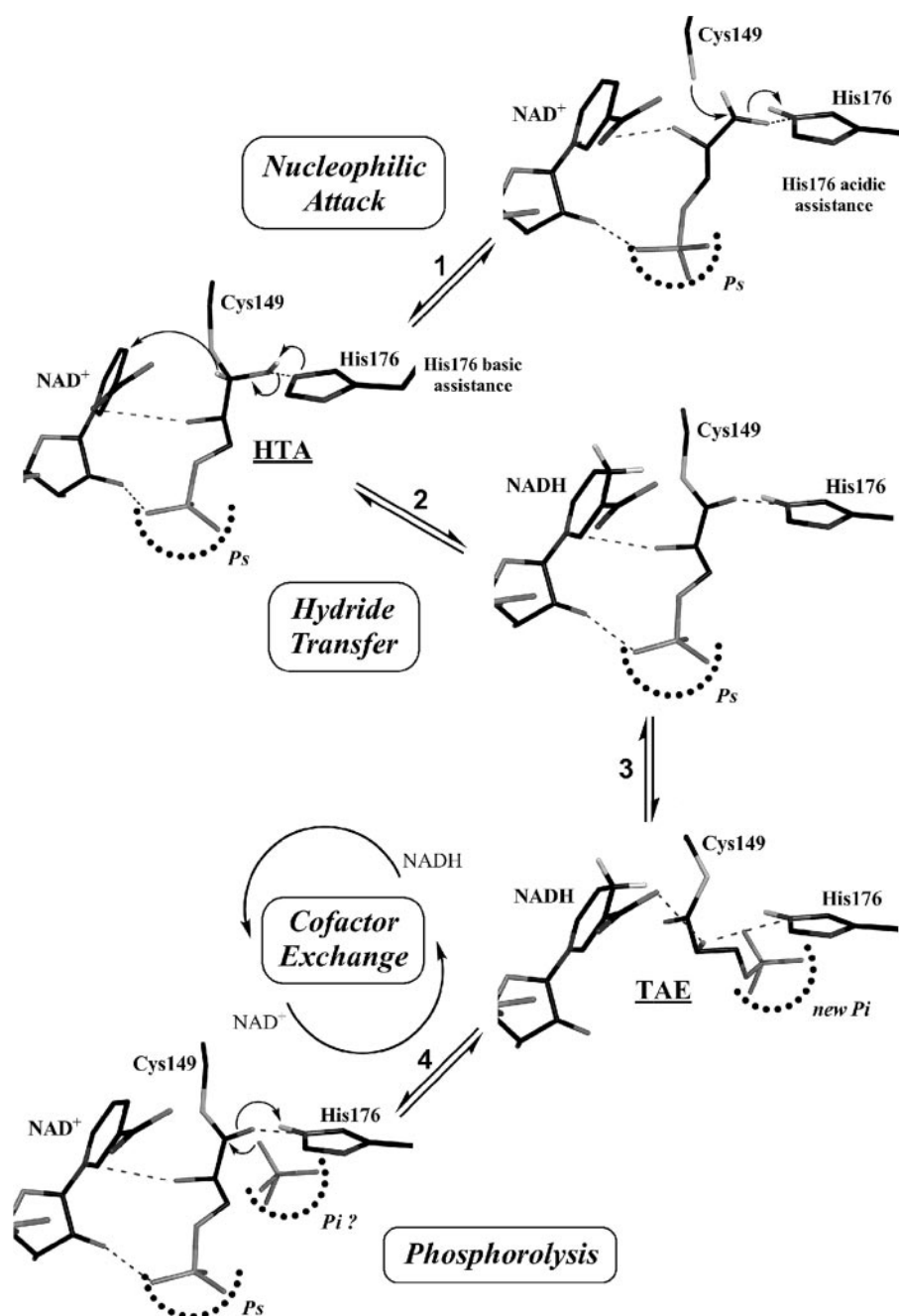


FIGURE 5. Structural scenario proposed for the catalytic mechanism. Only hydrogen atoms directly involved in the catalytic mechanism are represented. G3P initially binds to the active site of GAPDH with its C3P group located in the P_s site. Reaction begins through the nucleophilic attack of the Cys-149 thiolate function on the aldehydic carbon C1 of the substrate (*step 1*), which leads to a tetrahedral intermediate called hemithioacetal (*HTA*). This step is followed by hydride transfer (*step 2*), assisted by His-176, from the C1 atom of G3P to the C4 atom of NAD^+ . At this stage, C3P is thought to be located in the P_s site, and the O1 atom of G3P is expected to interact with His-176 (Ne) (see "Discussion"). To allow NADH release, the substrate must undergo a conformational change during which the orientation of the O1 atom changes while the C3P group flips toward the new P_i site (*step 3*). It results in the loss of the interaction between the substrate and the cofactor required for NADH release (*TAE*: thioacylenzyme intermediate corresponding to the structure depicted here). NAD^+ enters the active site and likely promotes the relocation of O1 and C3P to their initial position. The P_i site (either in the classic or new position, indicated as " $P_i?$ ") is free to bind an inorganic phosphate for the nucleophilic attack on the thioacylenzyme. This last step is also assisted by His-176 and leads to the formation of 1,3-bisphosphoglycerate. Subsequent release of the product leaves the enzyme in its holo-state, ready to accommodate a new G3P molecule.

activated through the formation of an ion pair with His-176, on the aldehydic carbon C1 of the substrate (Fig. 5, *step 1*). Hydride transfer occurs then from the C1 atom of the thiohemiacetal

intermediate to the C4 atom of the nicotinamide of NAD^+ through general base catalysis by His-176 (Fig. 5, *step 2*). At this stage, the C3P group of the thioacyl intermediate is likely still bound in the P_s site in close interaction with the cofactor (Fig. 5, *HTA stage*). Then, the thioacylenzyme intermediate undergoes conformational adjustments (Fig. 5, *step 3*) during which the orientation of the O1 atom changes in such a way that it now points away from His-176 while C3P flips toward the "new" P_i site. These events lead to the thioacylenzyme intermediate (Fig. 5, *TAE stage*) whose structure is presented here. The next step consists of the exchange of cofactor (NADH release, entry of a new molecule of NAD^+) (Fig. 5, *step 4*). Note that this step is facilitated by the loss of interaction between the substrate and the cofactor molecule due to the relocation of the C3P group in the new P_i site. The entry of a new NAD^+ molecule likely promotes conformational changes on the substrate molecule that are required for phosphorolysis, that is the flip back of both O1 atom and C3P group to their initial position. Inorganic phosphate finally binds to the active site and attacks the thioacylenzyme intermediate from the P_i site leading to product (1,3-DPG) release. At the end, the enzyme returns to its holo-form, ready to accommodate a new G3P molecule.

In this scenario, even if the thioacylenzyme structure presented here highlights the structural changes associated with the redox step, further work has to be carried out to understand how this putatively competent complex leads to 1,3-DPG formation. In that context, direct evidence is still lacking as to whether and/or how the redox state of the cofactor promotes the rearrangements required for the phosphorolysis step. In addition, the exact site from which inorganic phosphate attacks the thioacylenzyme intermediate is still speculative. The structure of a Michaelis-like complex with 1,3-DPG and NAD^+ , and of a thioacylenzyme- NAD^+ complex, will provide further information

Thioacylenzyme Intermediate from *B. stearotherophilus* GAPDH

regarding the mechanism of this “old” but still imperfectly known enzyme.

Acknowledgments—We thank Prof. G. L. Rossi for many stimulating discussions on GAPDH and microspectrophotometry. We gratefully acknowledge access to synchrotron radiation at the EMBL Outstation, Deutsches Elektronen-Synchrotron, Hamburg, and at the European Synchrotron Radiation Facility, Grenoble, France.

REFERENCES

1. Segal, H. L., and Boyer, P. D. (1953) *J. Biol. Chem.* **204**, 265–281
2. Trentham, D. R. (1971) *Biochem. J.* **122**, 59–69
3. Trentham, D. R. (1971) *Biochem. J.* **122**, 71–77
4. Harris, J. I., and Waters, M. (1976) in *The Enzymes*, 3rd Ed. (Boyer, P. D., ed) ch. 13, Academic Press, New York
5. Soukri, A., Mouglin, A., Corbier, C., Wonacott, A., Branlant, C., and Branlant, G. (1989) *Biochemistry* **28**, 2586–2592
6. Michels, S., Rogalska, E., and Branlant, G. (1996) *Eur. J. Biochem.* **235**, 641–647
7. Talfournier, F., Colloc'h, N., Mornon, J. P., and Branlant, G. (1998) *Eur. J. Biochem.* **252**, 447–457
8. Boschi-Muller, S., and Branlant, G. (1999) *Arch. Biochem. Biophys.* **363**, 259–266
9. Moras, D., Olsen, K. W., Sabesan, M. N., Buehner, M., Ford, G. C., and Rossmann, M. G. (1975) *J. Biol. Chem.* **250**, 9137–9162
10. Skarzyński, T., Moody, P. C., and Wonacott, A. J. (1987) *J. Mol. Biol.* **193**, 171–187
11. Korndörfer, I., Steipe, B., Huber, R., Tomschy, A., and Jaenicke, R. (1995) *J. Mol. Biol.* **246**, 511–521
12. Kim, H., Feil, I. K., Verlinde, C. L., Petra, P. H., and Hol, W. G. (1995) *Biochemistry* **34**, 14975–14986
13. Corbier, C., Michels, S., Wonacott, A. J., and Branlant, G. (1994) *Biochemistry* **33**, 3260–3265
14. Yun, M., Park, C. G., Kim, J. Y., and Park, H. W. (2000) *Biochemistry* **39**, 10702–10710
15. Castilho, M. S., Pavão, F., Oliva, G., Ladame, S., Willson, M., and Périé, J. (2003) *Biochemistry* **42**, 7143–7151
16. Didierjean, C., Corbier, C., Fatih, M., Favier, F., Boschi-Muller, S., Branlant, G., and Aubry, A. (2003) *J. Biol. Chem.* **278**, 12968–12976
17. Pearson, A. R., Mozzarelli, A., and Rossi, G. L. (2004) *Curr. Opin. Struct. Biol.* **14**, 656–662
18. Rossi, G. L., and Bernhard, S. A. (1971) *J. Mol. Biol.* **55**, 215–230
19. Mozzarelli, A., and Rossi, G. L. (1996) *Annu. Rev. Biophys. Biomol. Struct.* **25**, 343–365
20. Bourgeois, D., and Royant, A. (2005) *Curr. Opin. Struct. Biol.* **15**, 538–547
21. Berni, R., Mozzarelli, A., Pellacani, L., and Rossi, G. L. (1977) *J. Mol. Biol.* **110**, 405–415
22. Vas, M., Berni, R., Mozzarelli, A., Tegoni, M., and Rossi, G. L. (1979) *J. Biol. Chem.* **254**, 8480–8486
23. Mozzarelli, A., Berni, R., Rossi, G. L., Vas, M., Bartha, F., and Keleti, T. (1982) *J. Biol. Chem.* **257**, 6739–6744
24. Mozzarelli, A., Peracchi, A., Rossi, G. L., Ahmed, S. A., and Miles, E. W. (1989) *J. Biol. Chem.* **264**, 15774–15780
25. Kabsch, W. (1993) *J. Appl. Crystallogr.* **26**, 795–800
26. Evans, P. R. (1993) in *Proceedings of the CCP4 Study Weekend: Data Collection and Processing* (Sawyer, L., Isaacs, N., and Bailey, S., eds) pp. 114–122, Daresbury Laboratory, Warrington, UK
27. Vagin, A., and Teplyakov, A. (1997) *J. Appl. Crystallogr.* **30**, 1022–1025
28. Collaborative Computational Project, Number 4. (1994) *Acta Crystallogr. Sect. D Biol. Crystallogr.* **50**, 760–763
29. Murshudov, G. N., Vagin, A. A., and Dodson, E. J. (1997) *Acta Crystallogr. Sect. D Biol. Crystallogr.* **53**, 240–255
30. Emsley, P., and Cowtan, K. (2004) *Acta Crystallogr. Sect. D Biol. Crystallogr.* **60**, 2126–2132
31. Bricogne, G., and Irwin, J. J. (1996) in *Macromolecular Refinement. Proceedings of the CCP4 Study Weekends*, (Dodson, E., Moore, M., Ralph, A., and Bailey, S., eds) pp. 85–92 Daresbury Laboratory Warrington, UK
32. Laskowski, R. A., MacArthur, M. W., Moss, D. S., and Thornton, J. M. (1993) *J. Appl. Crystallogr.* **26**, 283–291
33. Ramakrishnan, C., and Ramachandran, G. N. (1965) *Biophys. J.* **5**, 909–933
34. Duée, E., Olivier-Deyris, L., Fanchon, E., Corbier, C., Branlant, G., and Dideberg, O. (1996) *J. Mol. Biol.* **257**, 814–838
35. Racker, E., and Krimsky, I. (1952) *J. Biol. Chem.* **198**, 731–743
36. Harrigan, P. J., and Trentham, D. R. (1974) *Biochem. J.* **143**, 353–363
37. Buehner, M., Ford, G. C., Moras, D., Olsen, K. W., and Rossmann, M. G. (1974) *J. Mol. Biol.* **82**, 563–585
38. Byers, L. D. (1978) *Arch. Biochem. Biophys.* **186**, 335–342
39. Cobessi, D., Tête-Favier, F., Marchal, S., Branlant, G., and Aubry, A. (2000) *J. Mol. Biol.* **300**, 141–152

Trapping of the Thioacylglyceraldehyde-3-phosphate Dehydrogenase Intermediate from *Bacillus stearothermophilus*: DIRECT EVIDENCE FOR A FLIP-FLOP MECHANISM

Sébastien Moniot, Stefano Bruno, Clemens Vornrhein, Claude Didierjean, Sandrine Boschi-Muller, Mária Vas, Gérard Bricogne, Guy Branlant, Andrea Mozzarelli and Catherine Corbier

J. Biol. Chem. 2008, 283:21693-21702.

doi: 10.1074/jbc.M802286200 originally published online May 14, 2008

Access the most updated version of this article at doi: [10.1074/jbc.M802286200](https://doi.org/10.1074/jbc.M802286200)

Alerts:

- [When this article is cited](#)
- [When a correction for this article is posted](#)

[Click here](#) to choose from all of JBC's e-mail alerts

Supplemental material:

<http://www.jbc.org/content/suppl/2008/05/14/M802286200.DC1>

This article cites 37 references, 11 of which can be accessed free at <http://www.jbc.org/content/283/31/21693.full.html#ref-list-1>